Journal of Advance Computational Research
Vol. 1 No. 1 (January-June, 2016)

A Practice of Smart Sensing System for Buried Mines Detecting based on Active Infrared Thermography Approach

Katsumi Wasaki
Faculty of Engineering, Shinshu University, 4-17-1 Wakasato Nagano-city, Nagano, Japan
E-mail: wasaki@cs.shinshu-u.ac.jp

Nobuhiro Shimoi
Department of Machine Intelligence and Systems Engineering, Faculty of Systems Science and Technology
Akita Prefectural University, 84-4 Aza Ebinokuchi Tsuchiya, Yurihonjo-city, Akita, Japan
E-mail: shimoi@akita-pu.ac.jp

Abstract: *This paper describes a smart remote sensing system that can detect scattered land mines by making use of an infrared (IR) camera. The proposed method uses parallel image processing based on time differences or subtracted images from the IR camera. Because of the danger involved, it is desirable for mines to be detected from as far away as possible. When mines are buried in the ground, we can detect them if there is a sufficiently large temperature gradient between the earth and the mine. First, cold water is sprayed over the surrounding region to cool the ground. By taking time-difference infrared images, objects buried in the soil will be detected because of their different cooling rates. Each subtraction image is processed in real time by using pipelined image-processing software implemented on an embedded Linux platform.*

Keywords: *Infrared Non-destructive Testing and Evaluation, Thermal Image Processing, Parallel Processing, Active Detection, Smart Sensing, Mine Detectors*

1. INTRODUCTION

Despite the end of the Cold War, as many as 80 million land mines are left buried today and are still killing or injuring many people all over the world [4]. Mines are designed to kill or wound people, so technologies for detection and disposal of mines must be safe and highly reliable. Figure 1 shows the exterior appearance of the Type-72A plastic mine. Sensing methods currently used for detecting mines buried underground include radar types (e.g., microwave pulse sensors, FM-CW and CW sensors) and magnetic types. However, because these sensors are housed in caster- or tire-type frames, their detection ability is adversely affected by vibrations transmitted from the ground surface during sensing and operation of these devices [16]. Figure 2 shows mine detection conducted with contact probes, but this detection method is extremely dangerous [7, 14].

When a mine is buried in the ground, it is possible to detect it if the peripheral temperature difference between the ground and the mine is large enough to sense (for a detailed description of related work, see Section 2) [11, 6, 5, 3, 10, 12].

We propose a smart sensing method for detecting land mines. Specifically, by using infrared (IR) thermography cameras, the work of detecting scattered mines can be done from a safe, remote location. Mine detection and disposal technologies will be improved by using measuring equipment based on IR cameras, and this will lead to active control remote sensing [15, 17].

With this system, we force the cooling of the ground surface by spraying a fixed amount of cold water over the mine area to produce a difference in radiant heat between the soil and the buried mine [8]. We have already confirmed that it is possible to detect mines using this radiant heat difference, if the temperature gradient between the ground and the mine is sufficiently large. We can measure the heat difference with an IR camera that is installed outside the mined region. By continuing measurements after the initial cooling, a sequence of time difference images is obtained from the changes in radiant heat and cooling speed. Next, by using an image-processing program running on an embedded Linux platform in this work, we can obtain the detection results of the buried objects in real time with a pipeline process. Human operators using this system can then study the position and condition of buried mines from a safe, remote location.

As one of the world's advanced nations in sensor technology, Japan should promote surveys and studies

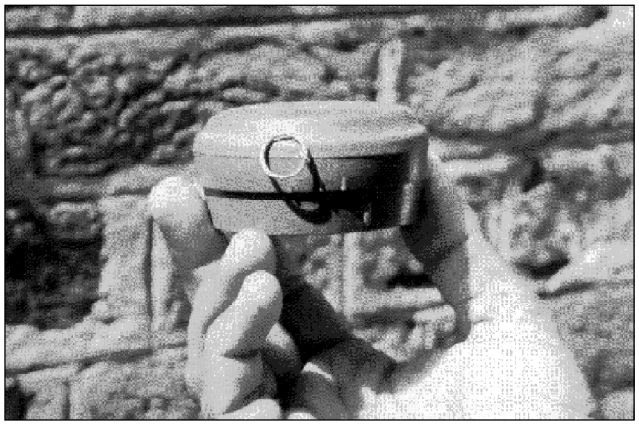

Figure 1: Type-72A Plastic Land Mine

Figure 2: Mine Detection using Contact Probes

on detecting mines safely using its advanced remote sensing technologies. We realize the urgency in proposing and promoting this research. This study focuses on the "object extraction" algorithm based on differences in cooling speed.

In contrast to conventional systems, which use fixed recognition techniques, our proposed system has several advantages:

- it uses feature extraction from time difference or subtraction images to inspect buried objects;
- it takes into consideration the condition of the ground, such as the proportions of stone, gravel and sand in the soil.

In fields such as character recognition, learning systems based on subspace methods are common. However, because the buried objects we want to detect are cylindrical forms or other similar shapes, it is unsuitable to use clustering learning based on differences in shape.

In the remainder of this paper, we first describe related work and the difficulties peculiar to mine detection. Then, we present the new inspection algorithm and image-processing software produced in this work. Finally, we state the results of the evaluation experiment using IR camera images that revealed mock mines.

2. RELATED WORK

In a number of inspection and detection applications, destructive control methods have been used to keep costs low. However, nondestructive testing and evaluation methods are being used more [2].

Because of the advantages of using infrared (IR) thermography, some applications dealing with the use of an IR camera as the major method of inspection and detection have already been published [1]. Since the 1990s, many techniques, tools and systems have been offered to enhance performance and accuracy based on passive and active thermography approaches. Kaplan [9] offers a complete review of the use of an IR imager as part of an inspection requirement.

In terms of detection and localization of hidden (i.e., buried) flaws in layered materials [10], some investigations have proposed and demonstrated the feasibility of thermographic evaluation. Wu [18] proposed, for example, a method of thermal contrast resistance to characterize subsurface features such as gaps or adhesion problems in veneered wood. Qin and Bao [13] also proposed a system for defect detection at the interface of the core in honeycomb structures in composite materials.

Alternatively, there are related studies of ground penetration radar (GPR), infrared (IR), or ultrasound (US) sensors for detecting buried mines. Assorted mine detection techniques are reviewed with particular emphasis on signal and image processing methods by Paik [12]. In this article, mines are categorized into two types: antitank mines (ATM) and antipersonnel mines (APM). For the signal processing and judgment modules, a set of image processing techniques including filtering, enhancement, feature extraction and segmentation were surveyed.

In the 1980s, a company released a product for the US military, "Infrared Scanning Cameras," to measure the spectral responses of two infrared camera systems [11]. In each system, the response was typical of the material from which the detector was made: indium antimonide (InSb) and mercury cadmium telluride (HgCdTe), respectively. Since the 1990s, a sensor fusion methodology has been studied for remote detection of buried land mines [6]. This primary approach was sensor

intrafusion and a dual-channel passive IR methodology that could distinguish true (fixed) surface temperature variations of 0.2 degrees from spatially dependent surface emissivity noise.

Studies of the effectiveness of stimulated infrared imaging in locating buried mines and mine-like objects have also been reported [3]. This work attempted to compare passive (that is, solar radiation-produced) images with those obtained using artificial stimulation, particularly high-power microwave (HPM) radiation. This method was, however, difficult to apply given the difficulties of electricity supply in developing countries.

A novel active infrared thermography approach, by spraying the soil to be inspected with water having a different temperature from the soil temperature, was proposed for land mine detection [5]. This simple approach produces different temperature zones to indicate the presence of buried mines. This work, related to pulsed thermography, was, however, limited to a simple simulation of the process.

We now state the problem description: to construct a machine vision system to detect buried flaws in layered material or ground by using active thermography. However, in most of these applications, the infrared images must be interpreted by a human expert. In this research, the machine vision system is automated and does not require any assistance from an operator.

3. FEATURE EXTRACTION FROM TIME-DIFFERENCE IMAGES

3.1 Temperature Measurement by IR Camera

Objects generally emit energy by infrared radiation [8]. Formula (1) shows the Planck radiation law:

$$W_b(\lambda) = \frac{2\pi hc^2}{\lambda^5\{\exp(hc/\lambda kt)-1\}} \times 10^{-5} \ [Watts/m^2.\mu m], \tag{1}$$

where the terms are:

$Wb(\lambda)$: the block body radiation spectroscope (λwave)

c : the velocity of light (=3×10^3 m/s)

h : Planck constant (= 6.6×10^{-34} J.s)

k : Boltzmann constant (= 1.4×10^{-23} J/K)

t : absolute temperature of the blackbody (K)

λ : the wavelength (m).

Formula (2) shows the Stefan–Boltzmann law for energy radiation [8]:

$$W_b - \sigma t^4 \ [\text{Watts} / m^2], \tag{2}$$

where the terms are:

W_b : the integral of $W_b(\lambda)$
: from wavelength $\lambda = 0$ to ∞

σ : the Stofan-Boltzmann constant
(= 5.7×10^{-8} Watts/m^2)

t : the absolute temperature of the blackbody (K).

From these equations, we find that the total energy emitted increases linearly with temperature, but the wavelength of the peak of the blackbody spectrum decreases. The only factor determining the radiation temperature is the blackbody temperature. For instance, at room temperature 20°C (circa 300 K) the energy distribution has a peak value at approximately 10μm. In addition, when considering absorption of radiation by the atmosphere, the wavelength ranges of 3 ~ 5μm and 8 ~ 12 μm are less attenuated by the atmosphere and can be considered suitable wavelengths for short-distance infrared rays. However, when we compare these two frequencies, the 8 ~ 12μm range is better for mine-detecting sensors than the 3 ~ 5μm range for IR imaging at room temperature.

3.2 Mine Detection Using Camera Images

Figure 3 shows an example of an IR camera image of a minefield. Almost all of the buried objects in this study are of a cylindrical shape. Because of the effect of stones in the soil, it is difficult to efficiently detect buried mines based on simple binary processing using threshold values. In addition, because ground temperature varies regionally, we must adjust the luminance level of (i.e., calibrate) the IR camera.

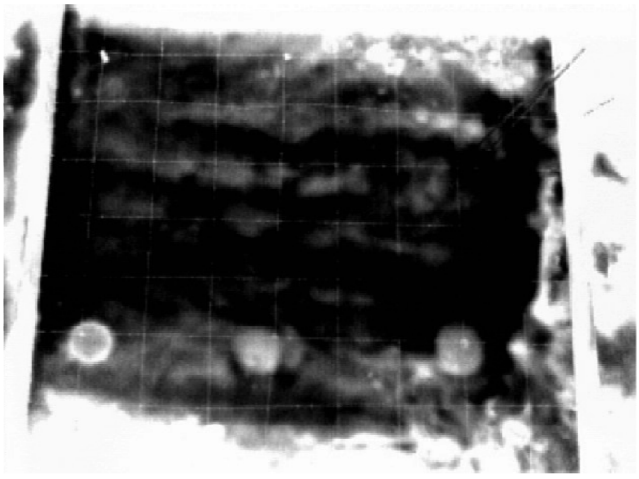

Figure 3: A Sample IR thermography Camera Image

We already know that it is possible to detect buried mines based on radiated heat when the peripheral temperature differences between the ground and mine objects are large enough to sense. However, there is a

problem because the "reverse phenomenon", in which the temperature of the ground begins to rise after the ground surface has cooled, occurs very quickly. Hence, when we measure the difference in temperature changes from IR camera images taken in a region outside the buried targets, a real-time method is required to process pictures before and after the reverse phenomenon.

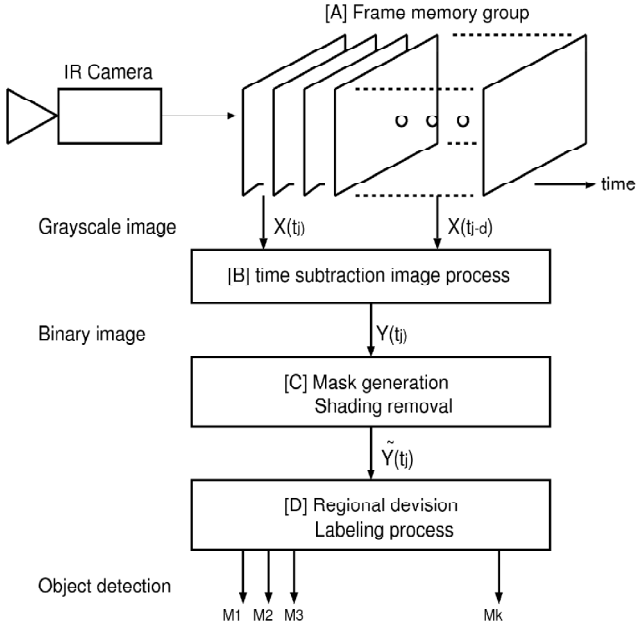

Figure 4: Configuration Diagram of the Detection-processing System

3.3 Proposed Detection Process

To examine the mine regions in this study, the images from the IR camera are recorded at a rate of one image frame per second and then input to the image-processing system. The test image photographs were created under the following conditions:

- imitate the actual survey situation as much as possible;
- conduct tests outdoors in fair weather; and
- install the IR camera 0.7 m away from the detection area.

Figure 4 shows the configuration diagram of the proposed detection-processing system. The processing is composed of four parts:

(A) a frame memory group for recording the time-elapsed images,

(B) time difference image processing,

(C) mask generation and shading removal, and

(D) division into regions and labeling.

(A) Frame Memory Group

The images from the IR camera are converted into 768 × 600-pixel grayscale pictures of 256 tones by the frame grabber hardware. Denote the horizontal width, vertical height and grayscale depth, respectively, as $Hw(=768)$, $Vw(=600)$ and $Gd(=256)$. This conversion process takes one second per image and each grayscale picture is stored in order in a FIFO-type frame memory of depth d.

For sampling times $t_0, t_1, \ldots, t_i, \ldots$, we define the images $X(t_i), X(t_{i-d}) \in X$ as the tail and head images in the frame memory at time t_i. Let $N_1 = \{0, 1, ..., Hw\}$ and $N_2 = \{0, 1, ..., Vw\}$. Then, we define a function μ as a mapping from $X \times N_1 \times N_2$ to the grayscale "pixel level" of the image as follows:

$$\mu : X \times N_1 \times N_2 \mapsto \text{level} \in \{0, 1,..., Gd-1\}$$
$$\mu(X(t), x, y) = \text{pixel value of image } X(t) \text{ at } (x,y) \quad (3)$$

We use two images $X(t_{j1}), X(t_{j2}), (i \le j2 < j1 \le d)$ from $X(t_i) \sim X(t_{i-d})$ in the frame memory group to make the time difference image for the next stage of processing.

(B) Time-difference Image Processing

By using the two images $X(t_{j1})$ and $X(t_{j2})$ taken from the frame memory at the previous stage, we determine the difference in intensity at the pixel level between the time (t_{j1}) at which the surface is cooled, and the measurement at the later time (t_{j2}).

For all pixels (x, y), the difference image $Y(t_{j2})$ is obtained by finding the difference in luminance level $\mu(X(t_{j1}), x, y)$ and $\mu(X(t_{j2}), x, y)$ at time t_{j1} and t_{j2}, respectively.

Definition 1 (Time difference image)

Let x, y be natural numbers such that $x \in Hw, y \in Vw$. *We define the function* $\mu(Y(t_{j2}), x, y)$

$$\rightarrow \textit{Element of } \{0, 1,..., Gd-1\}$$

$$= \begin{cases} \mu(X(t_{j2}), x, y) - \mu(X(t_{j1}), x, y) \\ \qquad (\textit{if } \mu(X(t_{j2}), x, y) > \mu(X(t_{j1}), x, y)) \\ 0 \\ \qquad (\textit{otherwise}) \end{cases} \quad (4)$$

This definition emphasizes the pixels that are at a substantially higher temperature (i.e., the luminance level is "*high*") after an elapsed time than at the time of ground surface cooling. On the other hand, for points with low or no temperature changes, for example, around stones on the surface or small pieces of refuse in the gravel, we

assign a luminance of zero. By creating the difference image in this way, we can reduce the noise in the mask generation and regional division process at the next stage and hence increase the detection rate of the mine objects.

(C) Mask Generation and Shading Removal

By using the difference images created in the previous stage, we make a region mask for setting the area of processing. Because most of the actual buried objects are cylindrical in nature, we can limit the object search to ellipses. However, it is difficult to achieve uniform cooling effects because of such influences as stones on the ground surface. As a result, there is a problem of shading around the object. For this, the following is assumed: (1) The top surfaces of the buried mines will be cooled almost uniformly. (2) The light transmitted will be observed from the ground level because the specific heat capacity of buried mines is large. Finally, we remove the shading effects of objects by normalizing the pixel $\mu(Y(t_{j2}), x, y)$ based on the average value $\mu(H(t_{j2}), x, y)$: = Average ($\mu(Y(t_{j2}), x, y), R$) of the neighborhood R of distance r from the pixel position $R = \{(x0, y0)$ s.t. $(x0, y0) \in B_{(x,y)}(r)\}$.

(D) Region Division and Labeling Process

After the removal of object image shading, we can generate a binary image $\tilde{Y}(t_{j2})$ with threshold Th ($0 < Th < Gd - 1$) using the following definition.

Definition 2 (Binary image)

Let x, y be natural numbers such that $x \in Hw$, $y \in Vw$.

We define the function $\mu(\tilde{Y}(t_{j2}), x, y)$

$$\rightarrow \textit{Element of } \{0,1\}$$

$$= \begin{cases} 1 & (\textit{if } \mu(X(t_{j2}), x, y) / \mu(H(t_{j2}), x, y) > Th) \\ 0 & (\textit{otherwise}). \end{cases} \tag{5}$$

Finally, for the binary image $\tilde{Y}(t_{j2})$, each target area in the mask $M_i \subseteq N_1 \times N_2$ ($i - 0, 1, ..., N_{max}$) is divided into regions using a raster scan-type labeling algorithm, and labels are assigned.

4. CONFIGURATION OF THE DETECTION SYSTEM

4.1 System Overview

Figure 5 shows the configuration of the land mine detection system using an IR camera. The results of measurements from the IR camera and processing signals are sent at the same time to the information-processing segment. A network connects this image processor and the operator's PC terminal. The proposed image-processing system is constructed from a standard IBM PC- compatible computer running the Linux operating system. On this machine, we implement the image-processing applications. Compared with specialized hardware for image processing, our system has some advantages in that it can be developed inexpensively with a high degree of flexibility for accommodating specification changes.

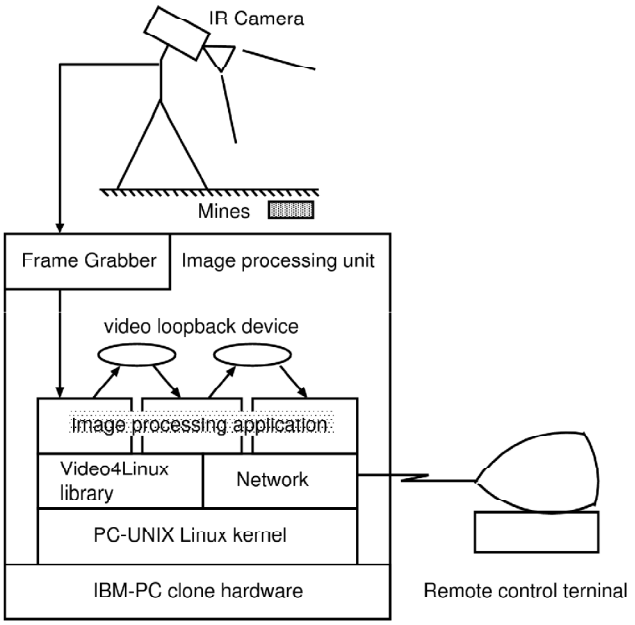

Figure 5: Functional Block Diagram of the Image-processing System

Because we use a standard embedded Linux-compatible computer, we also have the following benefits:

(1) it is easy to get replacement parts and supplies if there is a malfunction;

(2) with the speed-up of microprocessors, we can expect performance improvements in the future;

(3) because the Linux platform is an open system, there are no barriers placed by any country or enterprise to hinder development; and

(4) there is the possibility of promoting collaboration in developing applications for other countries.

Moreover, because this system uses the standard TCP/IP protocol and Ethernet physical layer, we can control and monitor multiple image processors connected via a network using the operation terminal.

4.2 Image-processing Unit

The applications for the image-processing segment described in the following were compiled using the GNU gcc optimizing compiler and linked against the Video4Linux library.

(a) Frame Grabber for Image Capture

First, we used a frame grabber add-in board on the PCI bus for image capture (Bt848 chipset, Brooktree Co.). This frame grabber is suited for use with the Video4Linux library and can accommodate any of the standard video formats (NTSC, PAL, SECAM) used around the world.

(b) Video4Linux Loopback Device

By using the loopback device function in the Video4Linux library, we constructed pipelined processing. The loopback device mechanism creates a virtual (internal) video device in the operating system that works as a virtual input/output capture device. For instance, to generate the frame memory group mentioned in Section 2, the frame grabber distributes images to the loopback device to balance the processing load.

(c) Image-processing Application Program

With a pipeline execution configuration, we can distribute the workload in a multiprocessor system for creating the region masks and the time-difference images. In general, a developer must divide the work to be done by each process by hand. By using the time-sharing multiplexing function of the Linux kernel, we succeeded in a natural division of load in the system. This effective utilization of system resources contributed to the realization of real-time processing.

(d) Networking and Remote Control Terminal

The image processor and the remote control terminal are connected by a network (wired or wireless Ethernet). The operator of the remote terminal determines the positions of the buried mines by using the detection and labeling results of image processing displayed on the terminal.

5. EXPERIMENT AND RESULTS

5.1 Experimental Methods

To evaluate the detection images, we constructed a wooden frame with a copper wire grid spaced 10 cm apart to verify the location of the buried mine targets. Figure 6 shows the experimental configuration.

On the day of experimentation, the weather conditions were moderate with a temperature of $32°C$. Mock mines were buried for one day and night in the sand and measurements began at 9:00 a.m. By using rain equipment, we sprinkled five liters of water, cooled to 4°C with ice, evenly on the ground surface of the area to be measured. Fifteen minutes of measurements were taken immediately. In this time, the image data were recorded by an $8 \sim 12\mu m$ band infrared camera (IR-U300M1) and a visual VTR camera to show the changing conditions. Thermocouples measured the change in temperature of the ground surface in the proximity of the buried mock mines. The buried mines were: $\phi 90 \times 45$ plastic ingot type, $\phi 70 \times 45$ plastic ingot type, $\phi 60 \times 120$ steel cylinder (containing $\phi 8 \times 150$ steel balls and 180g clay), buried at 2 and 1 cm depths.

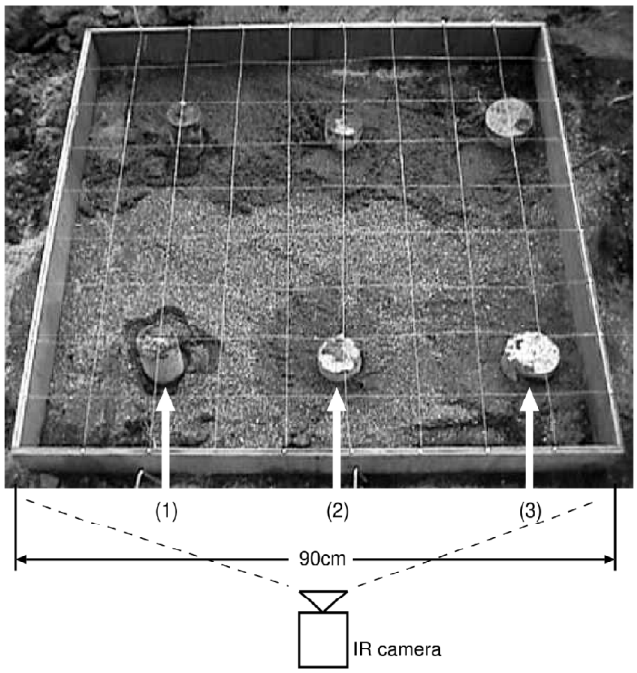

(a) Configuration of mock mine

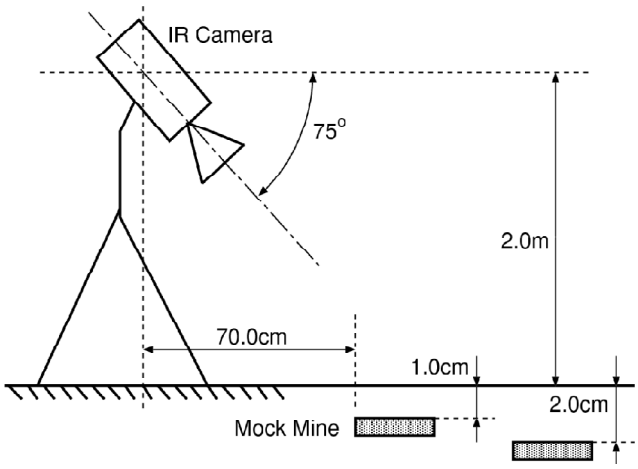

(b) Configuration of IR Camera

Figure 6: Experimental Configuration

5.2 Overall Evaluation of the Detection System

Figure 7 shows the two-dimensional temperature images of the mock mines taken by the infrared camera at selected intervals just after cooling the ground using the rain equipment. The coolant was sprinkled evenly over the ground surface where the mock mines were buried. For mines buried near the ground surface (1 cm depth), the images taken after the three-minute mark, (a), appeared the most clearly (see Fig. 3). After seven minutes, (b), the image became slightly indistinct and after 10 minutes, (c), it was no longer possible to distinguish the mine targets.

These results correspond to measurement results. The results agree with the theory that good mine location readings can be taken when the temperature gradient of the targets and the surrounding ground is large. In addition, for targets buried at 2 cm of depth, we could vaguely recognize the shape of mines from measurements taken at the 10- minute mark when the temperature difference was the greatest. The reason the result was not sufficiently good was because, compared with targets buried at 1 cm of depth, no sudden temperature changes could be detected from the thermometry results. Using these results, we applied the following image-processing techniques to try to enhance the mine detection information.

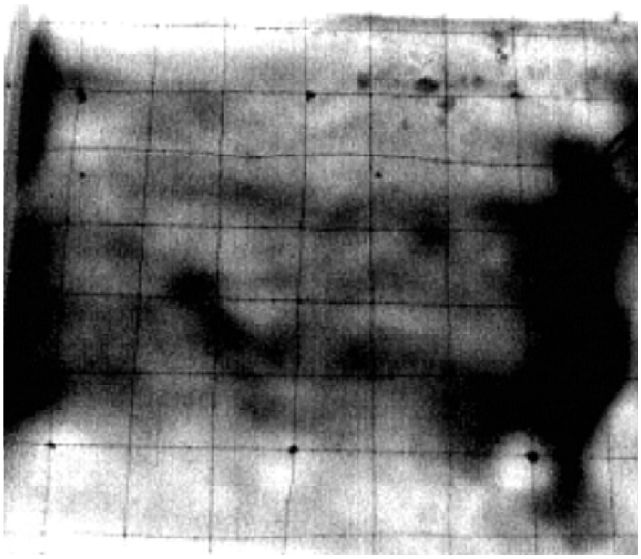

(c) After 10 minutes

Figure 7: Images from IR camera

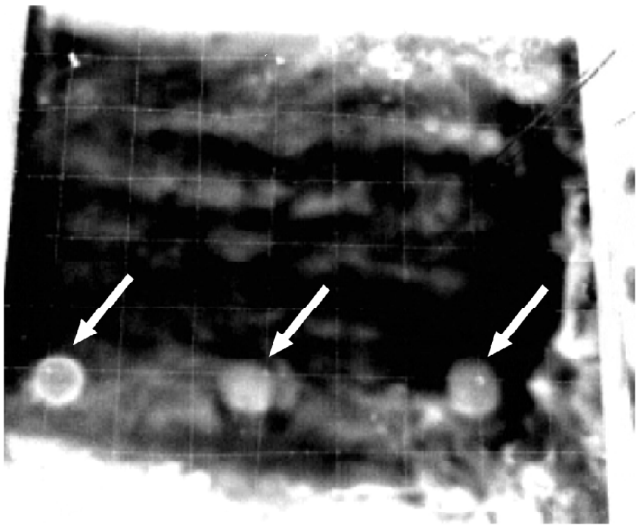

(a) After 3 minutes

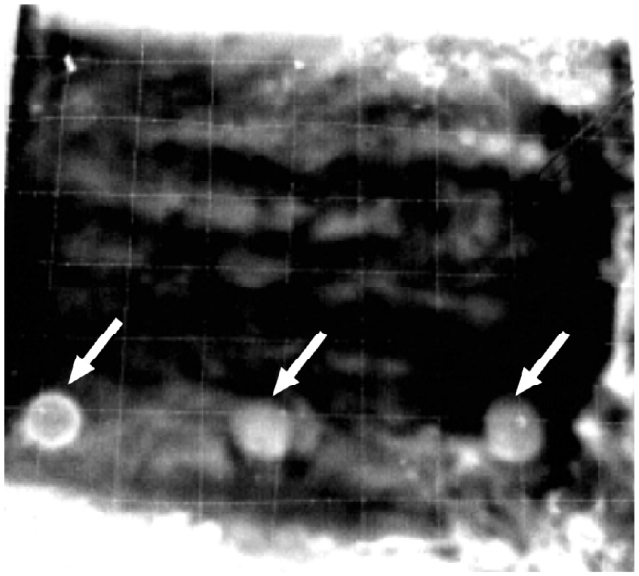

(b) After 5 minutes

Figure 8 shows the result of each step. Picture (a) shows the mine detection image from the IR camera (after seven minutes had elapsed). Picture (b) shows the result of the time difference image. Picture (c) is the binary image of the result using Th values for luminance level. Picture (d) shows the result of using regional division processing for a two-pixel radius Gaussian filter and then creating a binary image from it for Th levels of luminance. We then compared the changes resulting from these operations.

These results show that we can identify the location of all three buried mine targets where the image displays white spots. In addition, by studying image-processing technology, we can confirm the possibility of detecting mine targets buried at depths where normal recognition techniques have difficulties producing results. From the results of our work, the greatest merit of our active detection system using cooling water and infrared cameras is that operators can perform detection remotely, and thus more safely than with present metal detectors and radar sensors.

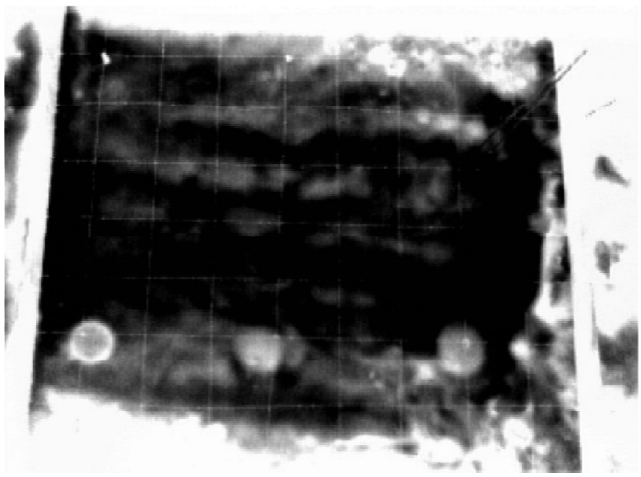

(a) Original picture

(c) Binary picture processing

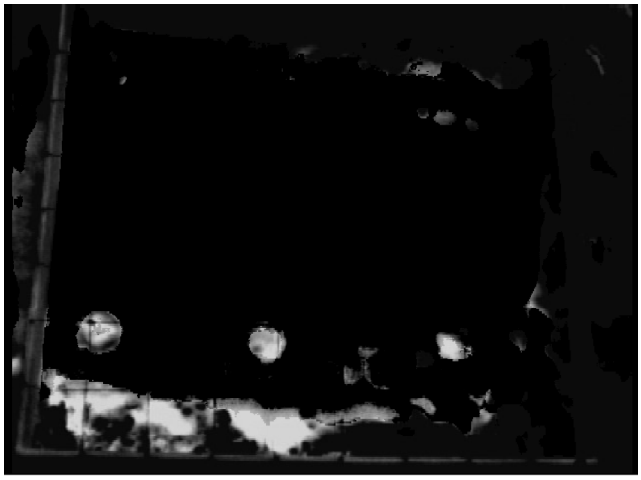

(b) Time difference image

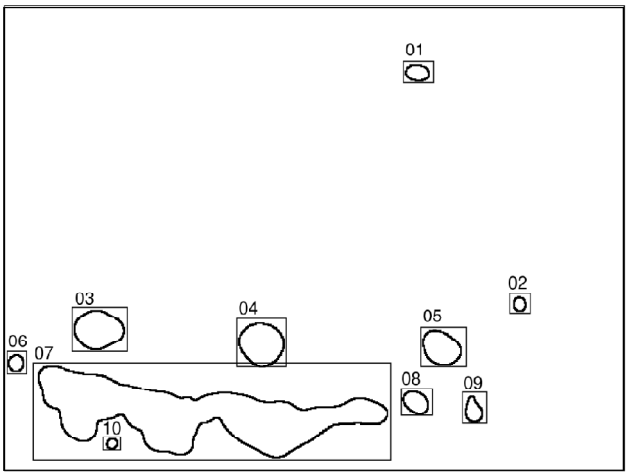

(d) Edge detection and image labeling

Figure 8: Image Processing of IR Scanning Results

From the standpoint of detection capacity, the results indicate that our system serves as an effective detector for buried land mines.

6. CONCLUSION

We have described the use of a smart sensing method for detecting land mines by using infrared ray thermography cameras. This method can detect scattered mines from a safe, remote location. For this purpose, our new detection method uses parallel image processing based on time differences or subtracted images from the IR camera. By spraying cold water over the surrounding region to cool the ground and taking time-difference infrared images, objects buried in the soil will be detected because of their different cooling rates. Each subtraction image has been successfully processed in real time by a pipelined image-processing system on an embedded Linux computer. Finally, we successfully realized a machine vision setup to detect buried flaws in layered material or the ground by using active thermography, with the capabilities to be interpreted automatically, without any assistance from an operator.

As one means of overcoming problems concerning lethal land mines we propose in this work the development of a mine detection system and demonstrate its potential. This work serves as a stepping stone for the development of mine removal technology for peaceful purposes. As one of the world's advanced nations in sensor technology, Japan should promote surveys and studies that will assist the work of detecting land mines safely by using its advanced remote sensing technologies. It is our hope that our small breakthroughs in mining research for humanitarian purposes will help researchers trying to find a way to save people suffering from injuries caused by mines.

ACKNOWLEDGMENT

We would like to express our thanks to Prof. Takita at the National Defense Academy and Mr. Osako at Mitsubishi Electric Incorporated for their assistance and cooperation during the outdoor experiments. This research was partially supported by the Ministry of Education, Science, Sports and Culture, Grant-in-Aid for Scientific Research(B)(1), 12450169, 1999–2001.

REFERENCES

[1] *15th Annual International Symposium on Aerospace Defense Sensing, Simulation; and Control, Aerosense, Thermo Sense*, Vol. XXII of *Proc. SPIE.*, Orlando, FL, USA, Apr. 2000.

[2] B. G. Batchelor, D. A. Hill, and D. C. Hodgson. Lighting and Viewing Techniques. In *Automated Visual Inspection*, Chapter 7. IFS Publications, North Holland, Amsterdam, 1986.

[3] L. J. Carter, A. Kokonozi, B. Hosgood, C. Coutsomitros, A. Sieber, and K. M. Hanson. Landmine Detection using Stimulated Infrared Imaging. In *Geoscience and Remote Sensing Symposium*, Vol. 3 of *Proc. IEEE.*, pp. 1110–1112, Jun. 2001.

[4] K. Furuta, K. Nonami, and N. Shimoi. The Study of Humanitarian Mine Detecting and Demining Technology. In *Science Council of Japan*, pp. 1–38. 2000.

[5] F. Galmiche and X. P. Maldague. Active Infrared Thermography for Land Mine Detection. In *Diagnostic Imaging Technologies and Industrial Applications*, Vol. 3827 of *Proc. SPIE.*, pp. 146–154, 1999.

[6] N. D. Grande. Sensor Fusion Methodology for Remote Detection of Buried Land Mines. In *Technical Report of National Symposium on Sensor Fusion*, pages 16–20. Lawrence Livermore National Lab., CA (USA), 1990.

[7] JCBL. Land Mine Monitor Report. In *Technical Report of Japan Land Mine Campaign Ban*, pp. 3–40. 1999.

[8] D. R. Jensen, S. G. Gathman, C. R. Zeisse, C. P. McGrath, G. de Leeuw, M. H. Smith, P. A. Frederickson, and K. L. Davidson. Electro-optical Propagation Assessment in Coastal Environments (eopace): Summary and Accomplishments. *Optical Engineering*, 40(8): 1486–1498, 2001.

[9] H. Kaplan. Practical Applications of Infrared Thermal Sensing and Imaging Equipment. In *Tutorials Texts in Optical Engineering. 2nd ed.*, Vol. TT34. SPIE Optical Engineering Press, Bellingham, WA, USA, 1986.

[10] A. C. Legrand, F. Meriaudeau, and P. Gorria. Active Infrared Non-destructive Testing for Glue Occlusion Detection within Plastic Lids. In *NDT and E International*, Vol. 35(3), pp. 177–187. Elsevier, 2002.

[11] Nacc. AGEMA : Infrared systems. In *Primer of Infrared Technology*, pp. 18–126. 1986.

[12] J. Paik, C. P. Lee, and M. A. Abidi. Image Processing-based Mine Detection Techniques: A Review. In *Subsurface Sensing Technologies and Applications*, Vol. 3(3), pp. 153–202. Springer, 2002.

[13] Y. W. Qin and N. K. Bao. Infrared Thermography and its Application in the ndt of Sandwich Structures. *Optics Lasers Engineering.*, 25: 205–211, 1996.

[14] N. Shimoi. The Subject ngo of the Technology for Mine Detecting. *Transaction on the Japan Society of Mechanical Engineers.*, B99-7:277–280, 1999.

[15] N. Shimoi, Q. Huang, H. Uchida, D. Komizo, and K. Nonami. The Smart Sensing for Mine Detection using ir Camera. In *Robotics and Mechatronics Symposium 2000*, Proc. JSME, pp. 93–94, 2000.

[16] N. Shimoi, S. Koga, and K. Itoh. Vibration Reduction Study with Air-cushion. *Transaction on Instrument and Control Engineers Japan.*, 35(5): 337–343, 1997.

[17] N. Shimoi, Y. Takita, K. Nonami, and K. Wasaki. Smart Sensing for Mine Detection Studies with ir Cameras. In *Computational Intelligence in Robotics and Automation*, Proc. IEEE, pp. 356–361, 2001.

[18] D. Wu. Lockin Thermography for Defect Characterization in Veneered Wood. In *Quantitative Infrared Thermography*, Vol. 42 of *Proceedings of Eurotherm Seminar*, pp. 298–302, 1994.